PAPER

Spatially selective hydrogen irradiation of dilute nitride semiconductors: a brief review

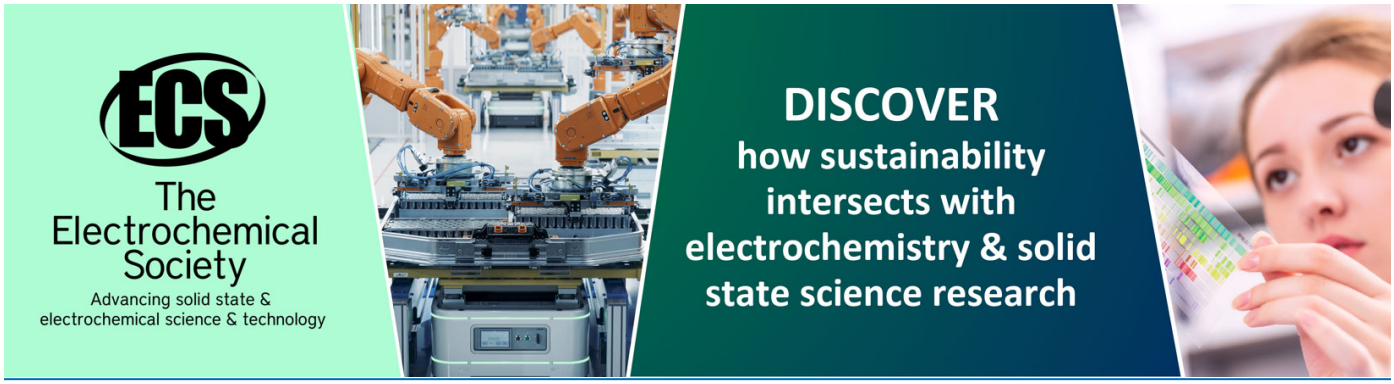

IOP Publishing Semiconductor Science and Technology
Semicond. Sci. Technol. 33 (2018) 053001 (8pp) https://doi.org/10.1088/1361-6641/aab3f1

Paper

Spatially selective hydrogen irradiation of dilute nitride semiconductors: a brief review

Marco Felici[1], Giorgio Pettinari[2], Francesco Biccari[3], Mario Capizzi[1] and Antonio Polimeni[1]

[1] Dipartimento di Fisica, Sapienza Università di Roma, I-00185 Rome, Italy
[2] National Research Council, Institute for Photonics and Nanotechnologies (IFN-CNR), I-00156 Rome, Italy
[3] Department of Physics and Astronomy, University of Florence, and LENS, I-50019 Sesto Fiorentino (FI), Italy

E-mail: marco.felici@roma1.infn.it

Received 6 February 2018, revised 27 February 2018
Accepted for publication 5 March 2018
Published 29 March 2018

Abstract

We provide a brief survey of the most recent results obtained by performing spatially selective hydrogen irradiation of dilute nitride semiconductors. The striking effects of the formation of stable N–H complexes in these compounds—coupled to the ultrasharp diffusion profile of H therein—can be exploited to tailor the structural (lattice constant) and optoelectronic (energy gap, refractive index, electron effective mass) properties of the material *in the growth plane*, with a spatial resolution of a few nm. This can be applied to the fabrication of site-controlled quantum dots (QDs) and wires, but also to the realization of the optical elements required for the on-chip manipulation and routing of qubits in fully integrated photonic circuits. The fabricated QDs—which have shown the ability to emit single photons—can also be deterministically coupled with photonic crystal microcavities, proving their inherent suitability to act as integrated light sources in complex nanophotonic devices.

Keywords: dilute nitrides, hydrogen in semiconductors, site-controlled quantum dots, nanophotonics

(Some figures may appear in colour only in the online journal)

1. Introduction - Hydrogen in dilute nitrides

Dilute nitride semiconductors, such as Ga(AsN), Ga(PN), and (InGa)(AsN), are III–V compounds containing small, yet macroscopic ($\leqslant$5%) percentages of nitrogen atoms within their lattice [1]. Although N has the same valence as the group-V atom it replaces, its incorporation in the host matrix results in a plethora of unexpected effects on the optoelectronic properties of this class of materials. While the huge, downward bowing of the energy gap [2] is probably the most technologically relevant effect of N incorporation in these compounds—in Ga(AsN) and in (InGa)(AsN) the ensuing redshift of the emitted photons allows approaching the 1.3 μm and 1.55 μm telecommunication windows, respectively—the strong perturbation exerted by the small, electronegative N atoms on the host lattice affects virtually every aspect of the electronic, optical, and structural properties of dilute nitrides, be it the electron effective mass [3, 4] and gyromagnetic factor [5], the lattice constant [6], the refractive index [7], or the electrical resistivity [8]. These striking effects mostly stem from the perturbation [9, 10] exerted on the band structure of the host by the strongly localized states associated with the excess charge surrounding N atoms, pairs and clusters [11–13].

What is perhaps even more striking, however, is the possibility to fully reverse these effects by *hydrogen irradiation* [14–21]: the exposure of the material's surface to a low-energy ($\sim$100 eV) flux of H ions results, indeed, in the

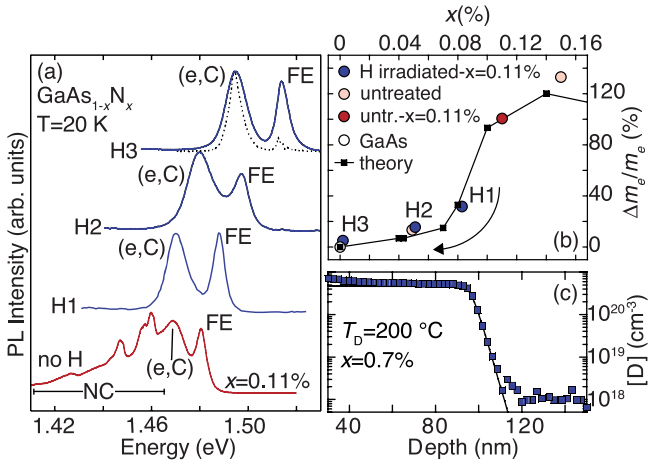

Figure 1. (a) Photoluminescence (PL) spectra at low temperature of untreated (red) and H-irradiated (blue) $GaAs_{1-x}N_x$ samples ($x = 0.11\%$, H1 $= 3.5 \times 10^{18}$ cm^{-2}, H2 $= 4.5 \times 10^{18}$ cm^{-2}, and H3 $= 5.0 \times 10^{18}$ cm^{-2}). The topmost dotted-line spectrum is recorded on a GaAs reference. FE and (*e*, *C*) indicate the free exciton and the free-electron to neutral-carbon recombination bands, respectively. NC indicates a quasi-continuum of states due to excitons recombining on various nitrogen complexes. (b) Percentage variation, $\Delta m_e/m_e$, of the electron effective mass m_e in $GaAs_{1-x}N_x$ as a function of x, as measured by magneto-PL [3]. The pink dots refer to untreated samples; the untreated $x = 0.11\%$ sample is highlighted in dark red, while the blue dots refer to the same sample hydrogenated with different H doses H1, H2, and H3 (see above). The open circle indicates the GaAs reference sample. The black squares are the calculated values of $\Delta m_e/m_e$ [23]. (c) Secondary-ion mass-spectrometry (SIMS) depth profile near the diffusion front of deuterium in a $GaAs_{1-x}N_x$ sample with $x = 0.7\%$, which underwent D irradiation at a temperature $T_H = 200$ °C. The solid line is the convolution of the diffusion profile—calculated as described in [24]—with the SIMS response function. Parts (a) and (b) were reprinted with permission from [23]. Copyright 2008 by the American Physical Society [23]; Part (c) is reprinted with permission from [24]. Copyright 2009 by the American Physical Society [24].

formation of N–*n*H ($n \geqslant 2$) complexes [22], which 'renormalize' the charge distribution around N atoms and neutralize all N-induced effects. As displayed in figure 1 [23, 24], this entails the possibility to finely tune the most relevant properties of these alloys—such as the energy gap (see figure 1(a)) and the electron effective mass (see figure 1(b))—between the value they have in the untreated sample and that typical of the N- free material. It is interesting to note that the N–2H complexes responsible for the passivation of the effects of N on the electronic properties [25] are remarkably stable; in Ga(AsN), thermal annealing experiments [6, 22, 26, 27] yield an activation energy of 1.89 eV [27], which results in the need to keep the sample at a temperature >300 °C for ⩾4 h in order to fully recover all the properties of the pristine alloy. This stability bodes well for the use of H-irradiated dilute nitrides in electrically driven devices, typically operating at temperatures below 50 °C–80 °C. Also of note, for photonic devices, is the possibility to locally break the N–H bonds by *light irradiation*. While this possibility certainly exists [28, 29]—and has been recently proposed, in connection with near-field illumination, as a mean to fabricate site-controlled nanostructures [30]—the power densities required to efficiently photodissociate the N–H complexes (~1 MW cm^{-2}) are several orders of magnitude higher than those required to properly excite single nanostructures in a photonic device (10–100 W cm^{-2}, see, e.g., [31]).

Most notably, however, the H-induced fine-tuning of the material's properties can be performed with very high spatial resolution, paving the way to the realization of site-controlled nanostructures and fully integrated optoelectronic devices by *spatially selective hydrogenation*. This enticing prospect is made possible by the peculiar 'box-like' shape of the H diffusion profile in dilute nitrides, an example of which is displayed in figure 1(c). As shown in the figure (which actually refers to the diffusion of *deuterium*, D, commonly employed in secondary-ion mass-spectrometry measurements in order to improve the signal-to-background ratio), such profile is characterized by a very sharp diffusion front (~5 nm/decade at a hydrogenation temperature $T_H = 200$ °C; ~10–15 nm/decade at $T_H = 300$ °C). As detailed in [24], this behavior—related to the formation of stable N–*n*H complexes [22], which in turn act as H *traps*—can be accurately modeled through an appropriate system of diffusion-reaction equations (in [24], the black line displayed in figure 1(c) was obtained by fitting the solution of such equations to the experimental data). In practical terms, however, such box-like diffusion profile entails that if a template for H incorporation is defined on the sample surface prior to H irradiation—for example by deposition of H-opaque masks [32]—the final H concentration map in the sample will accurately *follow that template*, thus resulting in a controlled spatial modulation of the material's properties. In the following two sections, we will present a brief overview of the main results obtained with this approach.

2. Strain and refractive-index engineering

While the effects of the interplay between the incorporation of N and H on the optical and electronic properties of dilute nitrides have rightfully garnered the most attention, the presence of these impurities in the host matrix also has important consequences on the structural properties of these materials. Indeed, the sizeable, N-induced reduction of the *lattice constant* of dilute nitrides—which mostly goes as predicted by the virtual crystal approximation [33]—is deeply affected by the formation of stable N–*n*H complexes in the material. In particular, while the N–2H complex responsible for the electronic passivation of N [25, 26] is associated with a full recovery of the lattice parameter of pristine GaAs, the formation of a N–3H complex—with the third H atom more loosely bound to N (an activation energy of 1.77 eV was estimated by thermal annealing [27])—is known to be responsible for an additional lattice expansion [6], resulting in a switch from tensile to compressive strain in hydrogenated Ga(AsN)/GaAs epilayers. As a consequence, the possibility to perform spatially selective hydrogenation can be exploited to carefully engineer the strain profile of the material (see figures 2(a), (b)), and, thus, the strain-dependent mixing between heavy-hole and light-hole *valence-band states*. In

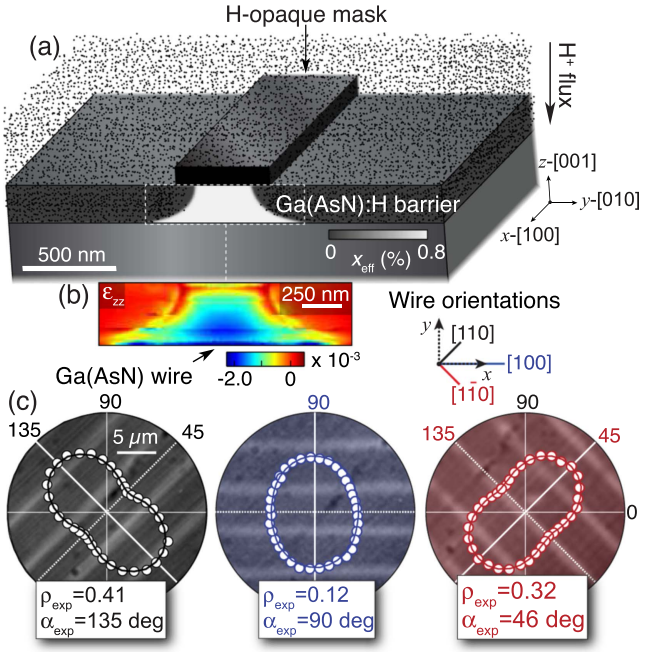

Figure 2. (a) Sketch of the process of spatially selective hydrogenation. Following the deposition of a H-opaque Ti mask, the sample is hydrogenated at a temperature $T_H = 300$ °C. The resulting $GaAs_{1-x}N_x$ wire is embedded in a (GaAs-like) $GaAs_{1-x}N_x$:H barrier (the wire is oriented along the [100] axis in the sketch). The effective N concentration (x_{eff}, corresponding to the concentration of unpassivated N atoms), displayed as a gray scale, results from finite-element calculations based on the model of H diffusion introduced in [24], and corresponds to a hydrogenation time of 10 000 s. (b) Spatial distribution (in the plane perpendicular to the wire) of the ε_{zz} component of the strain tensor in proximity of a $GaAs_{1-x}N_x$ wire ($x = 0.8\%$). (c) Polar plots of the micro-PL intensity ($T = 10$ K) of single $GaAs_{1-x}N_x/GaAs_{1-x}N_x$:H wires of different orientations, acquired as a function of the angle θ between the polarization vector and the [100] crystallographic axis. The experimental data points are plotted as circles, while fitting curves based on Malus's law are displayed as solid lines. The values of the degree (ρ_{exp}) and angle (α_{exp}) of linear polarization obtained from the fits are also reported for each wire orientation. The polar plots are superimposed to false-color micro-PL images (acquired at a temperature $T = 80$ K; the contribution of the substrate and of the hydrogenated barriers is filtered out with an 850 nm longpass filter) of the light emitted by wire arrays oriented at 45° (black), 0° (blue), and −45° (red) with respect to the [100] axis of the underlying crystal. Reprinted with permission from [34]. Copyright 2014 by the American Physical Society [34].

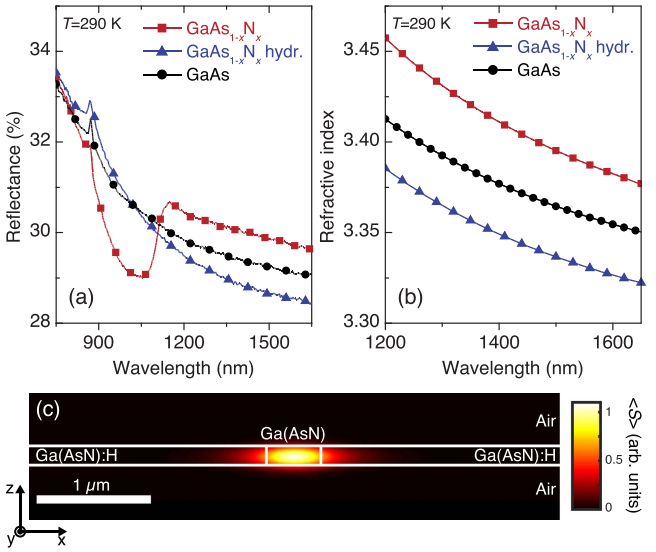

Figure 3. (a) Comparison of the room-temperature reflectance spectra of a GaAs reference (black dots) and of a $GaAs_{1-x}N_x$ sample ($x = 2.2\%$, thickness 100 nm) before (red squares) and after (blue triangles) H irradiation. (b) $GaAs_{1-x}N_x$ refractive index spectra before and after H irradiation, as obtained from the best fit to the reflectance spectra in the subgap region for the same sample shown in part (a) (the fitting procedure is detailed in [16]). The refractive index of GaAs is also shown as a reference. (c) Finite-elements calculation of the time-average of the Poynting vector, $\langle S \rangle$, computed (at a wavelength $\lambda = 1.3$ μm) for the fundamental mode of a 500 nm wide, 180 nm thick $GaAs_{1-x}N_x$ waveguide ($x = 2.2\%$), surrounded by air (top and bottom) and $GaAs_{1-x}N_x$:H (left and right). Parts (a) and (b) were reprinted with permission from [16] John Wiley & Sons. Copyright © 2012 WILEY-VCH Verlag GmbH & Co. KGaA, Weinheim.

turn, this allows for a fine-tuning of the optical properties of the material: by defining arrays of Ga(AsN)/Ga(AsN):H wires oriented at different angles [34], in particular, it was possible to achieve a high degree of linear polarization for the light emitted by the sample (see figure 2(c)). Furthermore, polarization-resolved micro-photoluminescence (PL) measurements revealed a non-trivial dependence on the wire orientation for both the polarization degree—going through a pronounced minimum for wires oriented along the [100] axis—and the polarization angle—precisely perpendicular to the wire when the latter is oriented along high-symmetry crystal directions, significantly tilted otherwise (see [34] for more details)—in excellent agreement with the predictions of a theoretical model based on Finite-Elements calculations. The possibility to adjust the polarization properties of dilute-nitride micro/nanostructures via H-assisted strain engineering might prove very useful when trying to optimize the performance of photonic devices based, e.g., on the polarization-dependent [35] coupling strength between dilute nitride-based light emitters and a *photonic crystal (PhC) microcavity*.

Within the context of nanophotonic applications, the possibility to tune the *refractive index*, *n*, of Ga(AsN) by hydrogen irradiation is obviously of particular importance. As already noted in the paragraphs above, indeed, the effects of hydrogenation on the band structure of dilute nitrides obviously have all-encompassing repercussions on the optical properties of these materials. While the reversal of the conduction-band redshift is clearly the most relevant effect of H irradiation in the region of the absorption edge—which is most easily characterized by absorption and/or photoluminescence excitation measurements [36, 37]—the formation of N–H complexes also affects deeply the behavior of dilute nitride semiconductors in the *sub-gap region*. As summarized in figures 3(a), (b), the effects of hydrogenation in this frequency range can be better appreciated by performing *reflectivity measurements*, which can then be fitted (as detailed in [7, 16]) to yield the refractive index of the material. As displayed in figure 3(b) (which refers to a 100 nm thick $GaAs_{1-x}N_x/GaAs$ epilayer with $x = 2.2\%$), in

the 1.2–1.6 μm spectral region the values of n measured in hydrogenated Ga(AsN) are systematically *lower* than those estimated for the untreated sample; actually, the effects of H on the refractive index seem to present an 'overshooting' phenomenon similar to that observed for the lattice constant, in the sense that in the H-irradiated material n does not match that of pure GaAs but dips further below through the entire wavelength range displayed in figure 3(b). As a result, untreated and hydrogenated Ga(AsN) are characterized by a nearly constant, ~2% refractive-index mismatch over a fairly broad wavelength interval, comprising both the 1.3 μm and the 1.55 μm telecommunications windows. As shown in figure 3(c), such mismatch is sufficient to tightly confine light within a sub μm-sized region: the finite-elements calculation displayed in the figure (performed at a wavelength $\lambda = 1.3$ μm) is based on a 500 nm-wide Ga(AsN) waveguide embedded in a Ga(AsN):H barrier (N concentration $x = 2.2\%$), which could be easily fabricated by employing the same masked-hydrogenation procedure used to realize the wires investigated in [34] (see also figure 2).

3. Quantum dot (QD) fabrication and integration with optical microcavities

As detailed in the previous section, the ability to engineer the refractive index of dilute nitrides with high spatial resolution might open the way to the realization of novel optical elements, useful for the manipulation and routing of light in nanophotonic circuits operating at the sub-wavelength level. Equally important, within this context, would be the possibility to integrate one or more light emitters at prescribed points of such photonic circuits. Ideally, the spatial and spectral position of these emitters should be controllable with a precision of a few nm; moreover, they should be able to generate non-classical light states 'on demand', i.e., exactly one photon [38] or one entangled photon pair [39] should be produced for each excitation pulse. In recent years, semiconductor QDs have emerged as particularly promising candidates for the realization of non-classical light emitters [40, 41], owing to their inherent integrability with optoelectronic devices as well as to continuous improvements in terms of their single-photon purity/indistinguishability and degree of entanglement [42–44]. The ability to control the position and emission energy of QDs has also made great strides in the past decade, due to the joint efforts of several research teams [31, 45–56]. Recently, the ability to modulate the band gap of dilute nitrides by spatially selective hydrogenation [32, 34], which we discussed in section 1, could be scaled down to the nm level thanks to the deposition of H-opaque masks having diameters $\leqslant$100 nm (as defined by *electron beam lithography*) [57–59]. As summarized in figure 4, this allowed for the development of an alternative approach to the fabrication of *site-controlled QDs* [57, 58], whose position and emission wavelength can both be controlled with a precision of ~20 nm. As shown in figure 4(c), these QDs also display the potential for triggered single-photon emission [58], thus making them ideal candidates for the deterministic integration

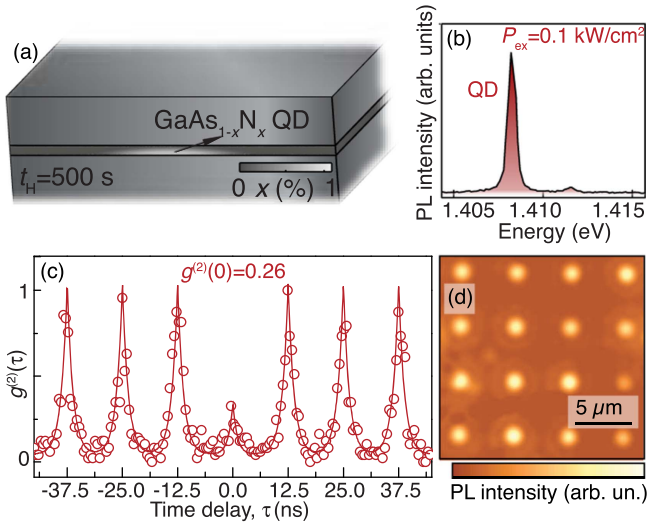

Figure 4. (a) Schematic lateral view of a sample embedding a $GaAs_{1-x}N_x/GaAs_{1-x}N_x$:H quantum dot (QD) fabricated by spatially selective hydrogenation. The spatial distribution of the concentration of non-passivated (i.e., not involved in the formation of the N–nH complexes responsible for N passivation) N atoms, displayed as a grayscale map, was obtained from Finite-Elements calculations of the H diffusion process in a masked sample (mask size 80 nm, hydrogenation temperature $T_H = 190$ °C, hydrogenation time $t_H = 500$ s), on the grounds of the model introduced in [24]. (b) MicroPL spectrum of a single $GaAs_{1-x}N_x/GaAs_{1-x}N_x$:H QD. (c) Normalized second-order correlation function, $g^{(2)}(\tau)$, for the excitonic emission of the QD whose micro-PL spectrum is displayed in (b). The amplitude of the central peak is well below the threshold value of 0.5, which points out to the emission of single photons by the QD. (d) Micro-PL image of a QD array, acquired by using a long wavelength pass filter to reject the GaAs emission. Reprinted with permission from [58]. Copyright 2014 American Chemical Society [58].

with nanophotonic devices, e.g., PhC microcavities. As sketched in figure 5(a), indeed, the H-opaque masks employed for the realization of Ga(AsN)/Ga(AsN):H QDs can be precisely aligned to a suitable set of reference markers, which can then be employed to center the position of an arbitrary photonic device with respect to the fabricated QD—or QDs. As summarized in figure 5, in [59] this procedure was applied to the realization of integrated QD-PhC cavity systems. The energy of the fundamental cavity mode (CM) of a series of *L3 photonic defects* (wherein the microcavity is obtained by removing three holes from an otherwise perfectly periodic photonic lattice [60]) was lithographically tuned into resonance with the QD emission by adjusting the lattice parameter of the PhC, a (see figure 5(b)). After achieving a coarse spectral matching between the CM and the QD exciton (X) for $a = 255$ nm, the system was progressively tuned into resonance by varying the sample temperature T, as displayed in figure 5(c). This is made possible by the much stronger T dependence of the energy of the X transition—which follows the band gap reduction of Ga(AsN) with T [61]—with respect to the CM, which linearly redshifts (at a rate of ~20 μeV K^{-1}, consistent with [62, 63]) due to the variation of the refractive index of GaAs with T. An interesting outcome of the progressive reduction of the QD-CM energy detuning with T is

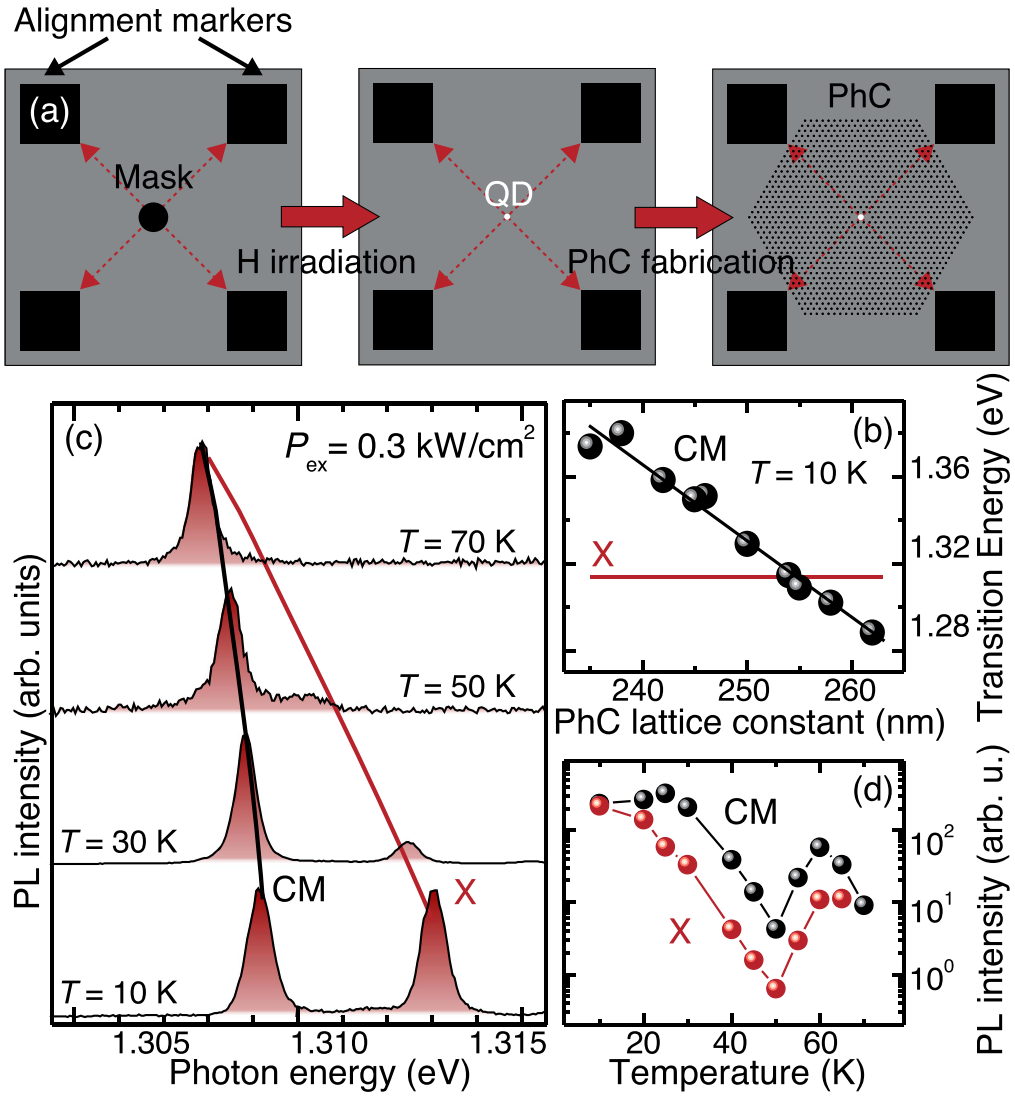

Figure 5. (a) Sketch of the steps leading to the deterministic integration of a single Ga(AsN)/Ga(AsN):H QD with a photonic crystal (PhC) cavity. First of all, an array of H-opaque masks is aligned to a set of metallic (chromium-gold) markers. Both the masks and the markers are defined by electron beam lithography. Second, H irradiation results in the formation of a site-controlled Ga(AsN)/Ga(AsN):H QD underneath each mask. Finally, a PhC cavity is fabricated around each QD. The reference system defined by the metallic markers ensures a near perfect (∼20 nm accuracy) alignment between the QD and the center of the PhC cavity. (b) Lithographic tuning of the cavity mode (CM) energy of a PhC L3 defect cavity by varying the value of the pitch, a, of the photonic lattice. The r/a ratio (where r is the radius of each PhC hole) is kept constant ($r/a = 0.29$). As expected, the dependence of the CM energy on a is ∼ linear, with $\frac{dE_{CM}}{da} \sim 3.5$ meV nm^{-1}. (c) Micro-photoluminescence (PL) spectra of an integrated QD-PhC cavity device, showing the temperature-dependent CM-QD detuning. The exciton transition of the QD is labeled as X. (d) Temperature dependence of the integrated PL intensity of the CM (black dots) and of the X peak (red dots). The intensity increase observed for temperatures above ∼50 K is a result of an increased QD-PhC cavity coupling (i.e., of the Purcell effect), due to the QD coming into resonance with the CM. Parts (b), (c), and (d) were reprinted from [59]. Copyright 2017 with permission from Elsevier.

reported in figure 5(d), which displays the temperature dependence of the micro-PL intensity of the QD and CM peak. As T is increased from 10 to 50 K, the PL signal shows the intensity drop-off usually expected in semiconducting samples, chiefly due to the thermal activation of non-radiative recombination channels [64]. For $T > 50$ K, however, a large increase in the PL intensity can be observed as the X line is moved into resonance with the CM. This is consistent with the ∼10-fold enhancement of the radiative recombination rate (the Purcell effect [65]) that was measured for this system (to be reported elsewhere [66]).

4. Outlook and conclusions

In summary, the possibility to modulate the optoelectronic properties of dilute nitride semiconductors by spatially selective hydrogenation might provide an ideal platform for the fabrication of fully integrated photonic circuits, embedding all the elements required for the generation, manipulation, and detection of non-classical light states within complex quantum computing schemes. In particular, the ability to control the refractive index of the material with sub-wavelength resolution (see section 2) will allow us to define

all the optical elements—such as waveguides, beam splitters and phase shifters [67]—required for the manipulation of photonic qubits. The site-controlled QDs fabricated by tailoring the energy gap of dilute nitrides *in their growth plane*, on the other hand, are very promising candidates for the on-chip generation of non-classical (e.g., single and entangled) photons (as discussed in section 3). The latter claim is further strengthened by recent progresses made in the realization [68, 69] and H irradiation [70, 71] of site-controlled (InGa)(AsN) nanostructures emitting in the 1.3 μm telecommunication window, which, as shown in figure 3, is well within the operating range of Ga(AsN)-based optical elements. The final piece of the puzzle, i.e., the on-chip detection of photonic qubits, will most likely rely on *superconducting-nanowire single-photon detectors* [72]. These detectors, which are characterized by high efficiencies, low dark-count rates, and ultra-fast response times, have been recently demonstrated to be fully compatible with GaAs-based photonic devices [73, 74] and are thus ideally suited for the integration with nanophotonic circuits relying on the concepts discussed in this work.

Acknowledgments

With regard to the research topics presented here, the Authors would like to acknowledge long-standing scientific collaborations with Rinaldo Trotta, Simone Birindelli, Annamaria Gerardino, Francesca Intonti, Anna Vinattieri, Massimo Gurioli, Gianluca Ciatto, Enrico Giulotto, and Mario Geddo. This work was supported by the Italian Ministry for Education, University and Research within the Futuro in Ricerca (FIRB) program (project DeLIGHTeD, Protocollo RBFR12RS1W). This work has also received funding from the European Union's Horizon 2020 research and innovation program under the Marie Sklodowska-Curie (grant agreement n. 641899), as well as by the 'Ateneo 2016' and 'Ateneo 2017' grants awarded by Sapienza University of Rome.

ORCID iDs

Marco Felici https://orcid.org/0000-0002-0977-2301

References

[1] Henini M 2005 *Dilute Nitride Semiconductors: Physics and Technology* (Oxford: Elsevier)
[2] Weyers M and Sato M 1993 Growth of GaAsN alloys by low-pressure metalorganic chemical vapor-deposition using plasma-cracked NH_3 *Appl. Phys. Lett.* **62** 1396–8
[3] Masia F *et al* 2006 Interaction between conduction band edge and nitrogen states probed by carrier effective-mass measurements in $GaAs_{1-x}N_x$ *Phys. Rev.* B **73** 073201
[4] Pettinari G, Polimeni A, Masia F, Trotta R, Felici M, Capizzi M, Niebling T, Stolz W and Klar P J 2007 Electron mass in dilute nitrides and its anomalous dependence on hydrostatic pressure *Phys. Rev. Lett.* **98** 146402
[5] Pettinari G *et al* 2006 Influence of nitrogen-cluster states on the gyromagnetic factor of electrons in $GaAs_{1-x}N_x$ *Phys. Rev.* B **74** 245202
[6] Bisognin G *et al* 2006 Hydrogen-nitrogen complexes in dilute nitride alloys: origin of the compressive lattice strain *Appl. Phys. Lett.* **89** 061904
[7] Geddo M *et al* 2007 Photoreflectance and reflectance investigation of deuterium-irradiated GaAsN *Appl. Phys. Lett.* **90** 091907
[8] Alvarez J, Kleider J-P, Trotta R, Polimeni A, Capizzi M, Martelli F, Mariucci L and Rubini S 2011 Giant and reversible enhancement of the electrical resistance of $GaAs_{1-x}N_x$ by hydrogen irradiation *Phys. Rev.* B **84** 085331
[9] Kent P R C and Zunger A 2001 Theory of electronic structure evolution in GaAsN and GaPN alloys *Phys. Rev.* B **64** 115208
[10] Lindsay A and O'Reilly E P 2004 Unification of the band anticrossing and cluster-state models of dilute nitride semiconductor alloys *Phys. Rev. Lett.* **93** 196402
[11] Thomas D G and Hopfield J J 1966 Isoelectronic traps due to nitrogen in gallium phosphide *Phys. Rev.* **150** 680
[12] Liu X, Pistol M E and Samuelson L 1990 Excitons bound to nitrogen pairs in GaAs *Phys. Rev.* B **42** 7504–12
[13] Felici M, Polimeni A, Miriametro A, Capizzi M, Xin H and Tu C 2005 Free carrier and/or exciton trapping by nitrogen pairs in dilute $GaP_{1-x}N_x$ *Phys. Rev.* B **71** 045209
[14] Polimeni A, Baldassarri G, Bissiri M, Capizzi M, Fischer M, Reinhardt M and Forchel A 2001 Effect of hydrogen on the electronic properties of $In_xGa_{1-x}As_{1-y}N_y$/GaAs quantum wells *Phys. Rev.* B **63** 201304
[15] Polimeni A, Bissiri M, Felici M, Capizzi M, Buyanova I, Chen W, Xin H and Tu C 2003 Nitrogen passivation induced by atomic hydrogen: the $GaP_{1-y}N_y$ case *Phys. Rev.* B **67** 201303
[16] Trotta R, Polimeni A and Capizzi M 2012 Hydrogen incorporation in III–N–V semiconductors: from macroscopic to nanometer control of the materials' physical properties *Adv. Funct. Mater.* **22** 1782–801
[17] Pettinari G, Felici M, Trotta R, Capizzi M and Polimeni A 2014 Hydrogen effects in dilute III–N–V alloys: from defect engineering to nanostructuring *J. Appl. Phys.* **115** 012011
[18] Ciatto G 2015 *Hydrogenated Dilute Nitride Semiconductors* (Singapore: Pan Stanford Publishing)
[19] Klar P J, Gruning H, Güngerich M, Heimbrodt W, Koch J, Torunski T, Stolz W, Polimeni A and Capizzi M 2003 Global changes of the band structure and the crystal lattice of Ga(N,As) due to hydrogenation *Phys. Rev.* B **67** 121206
[20] Polimeni A, Högersthal Von G B H, Bissiri M, Capizzi M, Frova A, Fischer M, Reinhardt M and Forchel A 2002 Role of hydrogen in III–N–V compound semiconductors *Semicond. Sci. Technol.* **17** 797–802
[21] Buyanova I *et al* 2004 Direct experimental evidence for unusual effects of hydrogen on the electronic and vibrational properties of GaN_xP_{1-x} alloys: a proof for a general property of dilute nitrides *Phys. Rev.* B **70** 245215
[22] Wen L, Stavola M, Fowler W B, Trotta R, Polimeni A, Capizzi M, Bisognin G, Berti M, Rubini S and Martelli F 2012 Microscopic origin of compressive strain in hydrogen-irradiated dilute $GaAs_{1-y}N_y$ alloys: role of N–Hn centers with $n > 2$ and their thermal stability *Phys. Rev.* B **86** 085206
[23] Polimeni A *et al* 2008 Role of strain and properties of N clusters at the onset of the alloy limit in $GaAs_{1-x}N_x$ *Phys. Rev.* B **77** 155213
[24] Trotta R, Giubertoni D, Polimeni A, Bersani M, Capizzi M, Martelli F, Rubini S, Bisognin G and Berti M 2009 Hydrogen diffusion in $GaAs_{1-x}N_x$ *Phys. Rev.* B **80** 195206

[25] Du M, Limpijumnong S and Zhang S 2005 Hydrogen pairs and local vibrational frequencies in H-irradiated $GaAs_{1-y}N_y$ *Phys. Rev.* B **72** 073202
[26] Berti M *et al* 2007 Formation and dissolution of D-N complexes in dilute nitrides *Phys. Rev.* B **76** 205323
[27] Bisognin G, De Salvador D, Napolitani E, Berti M, Polimeni A, Capizzi M, Rubini S, Martelli F and Franciosi A 2008 High-resolution x-ray diffraction *in situ* study of very small complexes: the case of hydrogenated dilute nitrides *J. Appl. Crystallogr.* **41** 366–72
[28] Balakrishnan N, Patanè A, Makarovsky O, Polimeni A, Capizzi M, Martelli F and Rubini S 2011 Laser writing of the electronic activity of N- and H-atoms in GaAs *Appl. Phys. Lett.* **99** 021105
[29] Balakrishnan N *et al* 2012 Band-gap profiling by laser writing of hydrogen-containing III–N–Vs *Phys. Rev.* B **86** 155307
[30] Biccari F *et al* 2018 Site-controlled single photon emitters fabricated by near field illumination *Adv. Mater.* accepted1705450
[31] Mohan A, Gallo P, Felici M, Dwir B, Rudra A, Faist J and Kapon E 2010 Record-low inhomogeneous broadening of site-controlled quantum dots for nanophotonics *Small* **6** 1268–72
[32] Felici M *et al* 2006 In-plane bandgap engineering by modulated hydrogenation of dilute nitride semiconductors *Adv. Mater.* **18** 1993–7
[33] Bisognin G, De Salvador D, Mattevi C, Berti M, Drigo A V, Ciatto G, Grenouillet L, Duvaut P, Gilet P and Mariette H 2004 Determination of lattice parameter and of N lattice location in $In_xGa_{1-x}N_yAs_{1-y}$/GaAs and GaN_yAs_{1-y}/GaAs epilayers *J. Appl. Phys.* **95** 48–56
[34] Felici M, Birindelli S, Trotta R, Francardi M, Gerardino A, Notargiacomo A, Rubini S, Martelli F, Capizzi M and Polimeni A 2014 Nanoscale tailoring of the polarization properties of dilute-nitride semiconductors via h-assisted strain engineering *Phys. Rev. Appl.* **2** 064007
[35] Calic M *et al* 2011 Phonon-mediated coupling of InGaAs/GaAs quantum-dot excitons to photonic crystal cavities *Phys. Rev. Lett.* **106** 227402
[36] Felici M, Trotta R, Masia F, Polimeni A, Miriametro A, Capizzi M, Klar P J and Stolz W 2006 Compositional disorder in $GaAs_{1-x}N_x$:H investigated by photoluminescence *Phys. Rev.* B **74** 085203
[37] Dudiy S V, Zunger A, Felici M, Polimeni A, Capizzi M, Xin H P and Tu C W 2006 Nitrogen-induced perturbation of the valence band states in $GaP_{1-x}N_x$ alloys *Phys. Rev.* B **74** 155303
[38] Michler P, Kiraz A, Becher C, Schoenfeld W V, Petroff P M, Zhang L D, Hu E and Imamoğlu A 2000 A quantum dot single-photon turnstile device *Science* **290** 2282–5
[39] Salter C L, Stevenson R M, Farrer I, Nicoll C A, Ritchie D A and Shields A J 2010 An entangled-light-emitting diode *Nature* **465** 594–7
[40] Lodahl P, Mahmoodian S and Stobbe S 2015 Interfacing single photons and single quantum dots with photonic nanostructures *Rev. Mod. Phys.* **87** 347–400
[41] Senellart P, Solomon G and White A 2017 High-performance semiconductor quantum-dot single-photon sources *Nat. Nanotechnol.* **12** 1026–39
[42] Huber D, Reindl M, Huo Y, Huang H, Wildmann J S, Schmidt O G, Rastelli A and Trotta R 2017 Highly indistinguishable and strongly entangled photons from symmetric GaAs quantum dots *Nat. Commun.* **8** 15506
[43] Somaschi N *et al* 2016 Near-optimal single-photon sources in the solid state *Nat. Photon.* **10** 340–5
[44] Schweickert L, Jöns K D, Zeuner K D, Covre da Silva S F, Huang H, Lettner T, Reindl M, Zichi J, Trotta R, Rastelli A and Zwiller V 2018 On-demand generation of background-free single photons from a solid-state source *Appl. Phys. Lett.* **112** 093106
[45] Felici M, Gallo P, Mohan A, Dwir B, Rudra A and Kapon E 2009 Site-controlled InGaAs quantum dots with tunable emission energy *Small* **5** 938–43
[46] Dalacu D *et al* 2009 Directed self-assembly of single quantum dots for telecommunication wavelength optical devices *Laser Photon. Rev.* **4** 283–99
[47] Surrente A, Gallo P, Felici M, Dwir B, Rudra A and Kapon E 2009 Dense arrays of ordered pyramidal quantum dots with narrow linewidth photoluminescence spectra *Nanotechnology* **20** 415205
[48] Huggenberger A, Heckelmann S, Schneider C, Höfling S, Reitzenstein S, Worschech L, Kamp M and Forchel A 2011 Narrow spectral linewidth from single site-controlled In(Ga)As quantum dots with high uniformity *Appl. Phys. Lett.* **98** 131104
[49] Surrente A, Felici M, Gallo P, Dwir B, Rudra A, Biasiol G, Sorba L and Kapon E 2011 Ordered systems of site-controlled pyramidal quantum dots incorporated in photonic crystal cavities *Nanotechnology* **22** 465203
[50] Schramm A, Tommila J, Strelow C, Hakkarainen T V, Tukiainen A, Dumitrescu M, Mews A, Kipp T and Guina M 2012 Large array of single, site-controlled InAs quantum dots fabricated by UV-nanoimprint lithography and molecular beam epitaxy *Nanotechnology* **23** 175701
[51] Jöns K D, Atkinson P, Müller M, Heldmaier M, Ulrich S M, Schmidt O G and Michler P 2013 Triggered indistinguishable single photons with narrow line widths from site-controlled quantum dots *Nano Lett.* **13** 126–30
[52] Liang B, Wong P-S, Tran T, Dorogan V G, Mazur Y I, Ware M E, Salamo G J, Shih C-K and Huffaker D L 2013 Site-controlled formation of InGaAs quantum nanostructures-tailoring the dimensionality and the quantum confinement *Nano Res.* **6** 235–42
[53] Holmes M J, Choi K, Kako S, Arita M and Arakawa Y 2014 Room-temperature triggered single photon emission from a III-Nitride site-controlled nanowire quantum dot *Nano Lett.* **14** 982–6
[54] Braun T, Schneider C, Maier S, Igusa R, Iwamoto S, Forchel A, Höfling S, Arakawa Y and Kamp M 2014 Temperature dependency of the emission properties from positioned In(Ga)As/GaAs quantum dots *AIP Adv.* **4** 097128
[55] Surrente A, Felici M, Gallo P, Dwir B, Rudra A, Biasiol G and Kapon E 2015 Polarization properties and disorder effects in H3 photonic crystal cavities incorporating site-controlled, high-symmetry quantum dot arrays *Appl. Phys. Lett.* **107** 031106
[56] Surrente A, Felici M, Gallo P, Rudra A, Dwir B and Kapon E 2017 Dense arrays of site-controlled quantum dots with tailored emission wavelength: growth mechanisms and optical properties *Appl. Phys. Lett.* **111** 221102
[57] Trotta R *et al* 2011 Fabrication of site-controlled quantum dots by spatially selective incorporation of hydrogen in Ga(AsN)/GaAs heterostructures *Adv. Mater.* **23** 2706–10
[58] Birindelli S, Felici M, Wildmann J S, Polimeni A, Capizzi M, Gerardino A, Rubini S, Martelli F, Rastelli A and Trotta R 2014 Single photons on demand from novel site-controlled GaAsN/GaAsN:H quantum dots *Nano Lett.* **14** 1275–80
[59] Pettinari G *et al* 2017 A lithographic approach for quantum dot-photonic crystal nanocavity coupling in dilute nitrides *Microelectron. Eng.* **174** 16–9
[60] Akahane Y, Mochizuki M, Asano T, Tanaka Y and Noda S 2003 Design of a channel drop filter by using a donor-type cavity with high-quality factor in a two-dimensional photonic crystal slab *Appl. Phys. Lett.* **82** 1341–3
[61] Polimeni A, Bissiri M, Augieri A, Baldassarri Hoger von Högersthal G, Capizzi M, Gollub D,

Fischer M, Reinhardt M and Forchel A 2002 Reduced temperature dependence of the band gap in $GaAs_{1-y}N_y$ investigated with photoluminescence *Phys. Rev.* B **65** 235325

[62] Gevaux D G, Bennett A J, Stevenson R M, Shields A J, Atkinson P, Griffiths J, Anderson D, Jones G A C and Ritchie D A 2006 Enhancement and suppression of spontaneous emission by temperature tuning InAs quantum dots to photonic crystal cavities *Appl. Phys. Lett.* **88** 131101

[63] Gallo P, Felici M, Dwir B, Atlasov K A, Karlsson K F, Rudra A, Mohan A, Biasiol G, Sorba L and Kapon E 2008 Integration of site-controlled pyramidal quantum dots and photonic crystal membrane cavities *Appl. Phys. Lett.* **92** 263101

[64] Pankove J I 1975 *Optical Processes in Semiconductors* (New York: Dover)

[65] Purcell E M 1946 Spontaneous emission probabilities at radio frequencies *Phys. Rev.* **69** 681

[66] Felici M *et al* Broadband enhancement of light–matter interaction in photonic crystal cavities integrating site-controlled Ga(AsN)/Ga(AsN):H quantum dots in preparation

[67] Crespi A, Osellame R, Ramponi R, Brod D J, Galvao E F, Spagnolo N, Vitelli C, Maiorino E, Mataloni P and Sciarrino F 2013 Integrated multimode interferometers with arbitrary designs for photonic boson sampling *Nat. Photon.* **7** 545–9

[68] Carron R, Fekete D, Gallo P, Dwir B, Rudra A, Felici M, Bartova B, Cantoni M and Kapon E 2011 Dilute nitride InGaAsN/GaAs V-groove quantum wires emitting at 1.3 μm wavelength at room temperature *Appl. Phys. Lett.* **99** 101107

[69] Carron R, Gallo P, Dwir B, Rudra A and Kapon E 2011 Dilute-nitride GaInAsN/GaAs site-controlled pyramidal quantum dots *Appl. Phys. Lett.* **99** 181113

[70] Felici M *et al* 2012 Magneto-optical properties of single site-controlled InGaAsN quantum wires grown on prepatterned GaAs substrates *Phys. Rev.* B **85** 155319

[71] Felici M *et al* 2012 Reduced temperature sensitivity of the polarization properties of hydrogenated InGaAsN V-groove quantum wires *Appl. Phys. Lett.* **101** 151114

[72] Gol'tsman G N, Okunev O, Chulkova G, Lipatov A, Semenov A, Smirnov K, Voronov B, Dzardanov A, Williams C and Sobolewski R 2001 Picosecond superconducting single-photon optical detector *Appl. Phys. Lett.* **79** 705–7

[73] Sprengers J P *et al* 2011 Waveguide superconducting single-photon detectors for integrated quantum photonic circuits *Appl. Phys. Lett.* **99** 181110

[74] Digeronimo G, Petruzzella M, Birindelli S, Gaudio R, Fattah Poor S, van Otten F and Fiore A 2016 Integration of single-photon sources and detectors on GaAs *Photonics* **3** 55